

1 **An Engineered Genetic Circuit for Lactose Intolerance Alleviation** 2 **Coupled with Gut Microbiota Recovery**

3 Mingyue Cheng^{1,2†}, Zhangyu Cheng^{1,2†}, Yiyan Yu^{1,2}, Wangjie Liu^{1,2}, Ruihao Li^{1,2}, Zhenyi

4 Guo^{1,2}, Jiyue Qin^{1,2}, Zhi Zeng^{1,2}, Lin Di^{1,2}, Yufeng Mo^{1,2}, Chunxiu Pan^{1,2}, Yuanhao Liang^{1,2},

5 Jinman Li⁴, Yigang Tong^{4,5}, Yunjun Yan^{1,3*}, Yi Zhan^{1,2,3*}, Kang Ning^{1,3*}

6 ¹ College of Life Science and Technology, Huazhong University of Science and Technology,

7 430074, Wuhan, P.R., China

8 ² Innovation Base of Life Science and Technology, Qiming College, Huazhong University of

9 Science and Technology, 430074, Wuhan, P.R., China

10 ³ Key Laboratory of Molecular Biophysics of the Ministry of Education, Huazhong

11 University of Science and Technology, 430074, Wuhan, P.R., China

12 ⁴ State Key Laboratory of Pathogen and Biosecurity, Beijing Institute of Microbiology and

13 Epidemiology, 100071, Beijing, P.R., China

14 ⁵ Beijing Advanced Innovation Center for Soft Matter Science and Engineering (BAIC-SM),

15 College of Life Science and Technology, Beijing University of Chemical Technology,

16 Beijing, 100029, Beijing, P.R., China

17 †These authors contributed equally to this work.

18 *Corresponding authors:

19 K. N.: ningkang@hust.edu.cn;

20 Y. Z.: zhanyi@hust.edu.cn;

21 YJ. Y.: yanyunjun@hust.edu.cn.

22 **Abstract**

23 **Background:** Lactose malabsorption occurs in around 68% of the world populations, causing
24 lactose intolerance (LI) symptoms such as abdominal pain, bloating and diarrhoea. To
25 alleviate LI, previous studies mainly focused on strengthening intestinal β -galactosidase
26 activity but neglected the inconspicuous colon pH drop caused by gut microbes' fermentation
27 on non-hydrolysed lactose. The colon pH drop will reduce intestinal β -galactosidase activity
28 and influence the intestinal homeostasis.

29 **Results:** Here, we synthesized a tri-stable-switch circuit equipped with high β -galactosidase
30 activity and pH rescue ability. This circuit can switch in functionality between expression of
31 β -galactosidase and expression of l-lactate dehydrogenase in respond to intestinal lactose
32 signal and intestinal pH signal. We confirmed the circuit functionality was efficient using 12-
33 hrs *in vitro* culture at a range of pH levels, as well as 6-hrs *in vivo* simulations in mice colon.
34 Moreover, another 21-days mice trial indicated that this circuit can recover lactose-effected
35 gut microbiota of mice to the status (enterotypes) similar to that of mice without lactose
36 intake.

37 **Conclusions:** Taken together, the tri-stable-switch circuit can serve as a promising prototype
38 for LI symptoms relief, especially by flexibly adapting to environmental variation, stabilizing
39 colon pH and restoring gut microbiota.

40 **Key words:** Lactose intolerance, Genetic engineering, Synthetic biology, Gut microbiota, *In*
41 *vitro* simulation, *In vivo* assessment

42

43 **Introduction**

44 The lactose malabsorption, defined as the inefficient absorption of lactose was reported to has
45 a global prevalence of 68%, which ranges from 28% in western, southern, and northern
46 Europe to 64% in Asia and 70% in the Middle East [1]. The regional prevalence is extremely
47 high in several countries requiring an efficient therapies such as 80% in Colombia (America),
48 85% in China (Asia), 98% in Armenia (Europe), 100% in South Korea (Asia), Yeman
49 (Middle East), and Ghana (Sub-Saharan Africa) [1]. Lactose intolerance (LI) symptoms,
50 defined as the presence of gastrointestinal symptoms caused by lactose malabsorption in the
51 small intestine, will occur when non-hydrolysed lactose flows into the colon as the bacteria
52 substrate [1, 2]. This non-hydrolysed lactose brings a high osmotic load into the colon
53 luminal contents, which leads to increased water and electrolytes followed by softening stool,
54 thus causing abdominal pain and cramps [3]. Meanwhile, this lactose can be fermented into
55 lactic acid and other short chain fatty acids with gaseous products such as hydrogen, CH₄,
56 and carbon dioxide, thus causing flatulence and diarrhoea [3, 4].

57 The current treatments for LI mainly include dietary control, enzyme replacement and
58 probiotic supplement. For dietary control, the moderation or restriction of lactose intake is
59 recommended to relieve symptoms [5–7], which impacts people’s enjoyment of dairy
60 products. Additionally, a recent study found that the administration of the highly purified
61 short-chain galactooligosaccharide can help to adjust gut microbiome to improve the LI [8].
62 Enzyme replacement is another important approach for large populations of LI individuals
63 [9]. The intake of exogenous lactase may help lactose digestion and absorption for LI

64 subjects, but its efficacy still lacks convincing evidence [2]. Compared to short-acting
65 enzyme replacement, probiotic supplements have an advantage in their sustainability [10] and
66 a certain number of studies have confirmed that they can alleviate LI [11–13]. The key
67 function of the probiotic is to enhance the intestinal β -galactosidase (β -GAL) activity of LI
68 individuals for lactose digestion. In addition, the endogenous β -GAL produced by the
69 probiotic is able to persist in a more stable manner in the intestine. However, the
70 conventional bacteria cannot deal with the pH drop caused by fermentation of gut microbiota.
71 The pH drop would not only cause physical discomfort such as diarrhoea, but also probably
72 reduce the β -GAL activity [14, 15], and influence the intestinal homeostasis.

73 Genetical engineering, which can make the precise control over genome sequence [16],
74 might be the solution for the pH drop problem faced by non-modified bacteria. Current
75 designs of engineered bacteria have been confirmed as effective through the development of
76 synthetic biology, for purposes such as infectious disease treatment [17] and cancer
77 diagnostics [18]. Moreover, bacteria engineered by synthetic biology are believed to work
78 more precisely and efficiently in addressing these diseases [19] compared to wild type
79 bacteria. Previously, a recombinant starin expressing food-grade β -GAL for LI was
80 constructed and evaluated [20, 21]. However, this engineered strain was still unable to deal
81 with the pH drop. A stress-responsive system might make the bacteria more adaptable to the
82 pH variation [22]. On the other hand, the influences of bacteria administration and pH drop
83 on gut microbiota remain unclear. The influences might be understood by observing
84 variations of gut microbiota during the lactose intake and bacteria administration phases.

85 In this study, we firstly designed and constructed a tri-stable-switch circuit using synthetic
86 biology in the plasmid *pet-28a-1* with two functional states (accumulation of β -GAL and pH
87 rescue) in response to signals of intestinal lactose and intestinal pH variation. Secondly, we
88 transformed the circuit into the strain *Escherichia coli* BL21 (*E. coli* BL21) to form the
89 engineered strain BL21: *pet-28a-1*, which was then used to confirm the circuit functionality
90 *in vitro* and *in vivo*. Lastly, we investigated on variation of mice gut microbiota and found
91 that the administration of engineered strain BL21: *pet-28a-1* can recover mice gut microbiota
92 affected by excess lactose intake.

93

94 **Results**

95 **The tri-stable-switch circuit can switch between two functionalities in response to** 96 **environmental change**

97 The tri-stable-switch circuit in the plasmid *pet-28a-1* (Fig. 1a, Additional file 2: Table S1 and
98 Additional file 3) was designed based on a tri-stable switch derived from bacteriophage
99 *lambda* [23]. The mutant lactose-inducible promoter placm (Additional file 2: Table S1) and
100 pH-responsive promoter *patp2* (Additional file 2: Table S1) were applied to sense the signal.
101 The key enzymes applied within the system were the products of *lacZ* (β -galactosidase, β -
102 GAL) and the fusion gene *ompA-ldd* (L-lactate dehydrogenase, L-LDH). To confirm the
103 functionality of the circuit, we choose the strain *Escherichia coli* BL21 as the chassis which
104 has been commonly used for stable expression of nontoxic exogenous protein. The circuit
105 was transformed into the strain *Escherichia coli* BL21 (*E. coli* BL21) to form the engineered

106 strain BL21: *pet-28a-1*. BL21: *pet-28a-1* was then able to dynamically switch between two
107 functional states, which was regulated by lactose signal and pH signal: accumulation of β -
108 GAL to digest lactose, and expression of L-LDH to rescue pH drop.

109 BL21: *pet-28a-1* can accumulate β -GAL after it colonized the colon (Fig. 1b). The mean
110 pH of 7.0 in the human colon [24], as a signal, maintained continuous *cI* expression by
111 inducing promoter *patp2*. The *cI* expression, which could hinder the transcripts of the gene
112 after pR [25], then suppressed expression of *ompA-lldD* and *cIII*, thus ceasing the function of
113 pH rescue. At this moment, the engineered bacteria would focus on the expression of the *lacZ*
114 and accumulate β -GAL for supplementary lactose digestion when unabsorbed lactose fluxed
115 into the colon.

116 BL21: *pet-28a-1* would gradually switch from *lacZ* expression to *ompA-lldD* expression
117 after lactose fluxed into the colon (Fig. 1c). On the one hand, the lactose as a signal would
118 trigger the promoter *placm*, thus activating the positive feedback loop of pRE, *cro* and *cII*.
119 The *cro* expression then began to suppress the *lacZ* expression after the pRM through binding
120 to its binding site [25]. Additionally, the *cro* expression can be strengthened by the *cII*
121 expression. Nevertheless, owing to the suppression on the *cII* expression by endogenous *Ftsh*
122 expression [26], this strengthening was suppressed to a certain degree. On the other hand,
123 fermentation of lactose by gut microbiota would produce lactic acid and other short chain
124 fatty acids, leading to acute drop of pH in the colon. This pH drop would weaken the *patp2*,
125 suppressing the *cI* expression. However, the previous expressed products of *cI* would still
126 suppress the expression of *ompA-lldD* and *cIII* to a certain degree, the suppression of which

127 would gradually diminish because of degradation of these products. Hence the *ompA-lldD*
128 expression would gradually recover to a normal condition, producing a signal peptide [27]
129 and L-LDH [28, 29], which would be translocated on the cell membrane to transform lactic
130 acid to pyruvate in the periplasm. In the meantime, the gradually recovered *cIII* expression
131 would eliminate the suppression on *cII* expression by suppressing endogenous expressed *Ftsh*
132 [26]. The unsuppressed *cII* expression then strengthened the *cro* expression, thus accelerating
133 the cease of *lacZ* expression. Together, at the beginning of the period when lactose fluxed
134 into the colon, the whole system was in an intermediate state of double functions. This was
135 caused by the signals brought activation and deactivation of the pathways as well as the
136 remained products such as repressor proteins which were not timely degraded.

137 Once these products were degraded, the BL21: *pet-28a-1* would then focus on *ompA-lldD*
138 expression (Fig. 1d). The suppression on expression of *cIII* and *ompA-lldD* would be
139 removed. On the one hand, constitutively expression of *cIII* eliminated the suppression on *cII*
140 expression by endogenous expressed *Ftsh*, thus keeping lactose-activated positive feedback
141 loop working to cease the *lacZ* expression. On the other hand, the *ompA-lldD* expression kept
142 producing efficient signal peptides and L-LDH to transform lactic acid to pyruvate to rescue
143 the pH drop (Fig. 1e). Afterwards, the pyruvate was transported into the cell by its carrier
144 protein [30, 31] for the tricarboxylic acid (TCA) cycle [32]. Together, in this round of lactose
145 intake, the engineered bacteria finished the lactose digestion as well as pH rescue.

146 BL21: *pet-28a-1* would subsequently switch to β -GAL accumulation for the next round of
147 lactose ingestion. In this way, the BL21: *pet-28a-1* would switch back and forth in response
148 to pulsed lactose intake.

149 **The tri-stable-switch circuit was efficient under a range of pH simulation *in vitro***

150 The promoters and transcriptional factors of the circuit have been tested by fluorescence
151 detection (Additional file 1: Supplementary methods, Additional file 2: Table S2 and Table
152 S3). We then tested whether the whole circuit can work effectively *in vitro* and *in vivo*. In the
153 *in vitro* experiment (Fig. 2), we prepared mediums of three pH sets with 0.1% lactic acid and
154 1% lactose (Additional file 1: Supplementary methods) to simulate the pH range of acidic
155 conditions caused by excess lactose intake in the human colon, whose normal pH is around 7
156 [24], as well as the mice colon, whose normal pH is around 5 [33]. Three pH sets included
157 pH set I (initial pH = 4.54 ± 0.012), pH set II (initial pH = 5.34 ± 0.02), and pH set III (initial
158 pH = 6.25 ± 0.02).

159 We subsequently recorded the variation of pH values and the expressed enzyme activity
160 (Additional file 2: Table S5) during the following 12-hrs culturing of the bacteria at three pH
161 levels, including the control strain (BL21: *pet-28a-0*) and the test strain (BL21: *pet-28a-1*). In
162 addition, the control strain BL21: *pet-28a-0* (Additional file 4) was the *E. coli* BL21
163 transformed with empty vector. As was shown in Fig. 2a, pH values of the control culture and
164 the test culture begin to increase at 6h. The increase of pH in the control culture was mainly
165 associated with two processes including the metabolism of the massive increase of the
166 bacteria and the consumption of the medium, while there was another additional process in

167 the test culture that the expressed L-LDH helped to digest the lactic acid to increase pH. The
168 additionally increased pH caused by L-LDH process was evident in the pH set I: The pH of
169 the test culture increased to a higher degree than that of the control culture (test culture: 4.54
170 ± 0.02 to 5.31 ± 0.075 ; control culture: 4.54 ± 0.01 to 4.9 ± 0.072). The additionally
171 increased pH in the test culture was observed in the pH set II and III as well, though not as
172 obvious as that in the pH set I.

173 As was shown in Fig. 2b and c, the β -GAL activity and L-LDH activity of the test group
174 were higher than those of the control group, which was caused by the expression of the *lacZ*
175 gene and *ompA-lldD* gene of the circuit in the BL21: *pet-28a-1*. Before 4h, the measures for
176 enzyme activity was unavailable because of the minimal amount of bacteria. After 4-hrs
177 culturing, the β -GAL activity of the test group kept increasing stably in all three pH sets. In
178 addition, from 8h to 10h in pH set II and pH set III, the β -GAL activity of the test group
179 increased to the greatest extent and later flattened. In the other hand, the L-LDH activity of
180 test group began to decrease in pH set II and pH set III after 10-hrs culturing. The
181 corresponding pH range of the test group during 8h to 10h was 6.43 ± 0.10 to 7.23 ± 0.07 in
182 pH set II, and 6.58 ± 0.03 to 7.34 ± 0.07 in pH set III, which meant that the switch of the
183 functionality of the circuit was completed in this pH range. These results suggested that the
184 relatively low pH promoted the L-LDH expression of the circuit to remove the lactic acid for
185 increasing pH, and the increased pH can make the circuit begin to switch gradually from L-
186 LDH expression to β -GAL expression, which would be completed in a pH range close to a
187 neutral condition.

188 **The tri-stable-switch circuit helped mice to recover the pH drop caused by excess**

189 **lactose intake**

190 The *in vitro* experiment has confirmed the theoretical feasibility of the tri-stable-switch
191 circuit to alleviate LI by switching between β -GAL expression and L-LDH expression, while
192 whether it can work in *in vivo* still remained unclear. We thus recruited 84 mice, divided into
193 five groups including the Initial set (n = 4), the Untreated group (n = 20), the Model group (n
194 = 20), the Control group (n = 20), and the Test group (n = 20) to investigate on how the
195 circuit worked *in vivo*. As was shown in Fig. 3a, in the first one week, mice in the Control
196 group and the Test group were daily administrated with bacteria (BL21: *pet-28a-0* in the
197 Control group, BL21: *pet-28a-1* in the Test group. OD₆₀₀ = 1) in a total volume of 0.3 mL
198 0.9% NS suspension. The bacteria have been confirmed to colonize the mice colon, which
199 can last at least 24 hrs (Additional file 1: Supplementary methods). Other groups were daily
200 administrated with the same volume of NS. At 0h, mice of the Initial set were killed to test
201 colon pH values as the pH value at 0h for all groups, and mice of other four groups were
202 administrated with the lactose solution (12 mg of lactose per 20 g of body weight). In the
203 following six hrs, the pH values of mice colons of the remained four groups were tested at
204 each time point (Additional file 2: Table S6), and then plotted in Fig. 3b to show the pH
205 variation. It was observed that the colon pH value of the Model group and the Control group
206 evidently decreased to 4.66 ± 0.15 and 4.72 ± 0.25 from 0h to 3h, respectively, and then
207 recovered to 4.89 ± 0.24 and 4.94 ± 0.1 from 0h to 3h, respectively. However, the colon pH
208 value of the Untreated group without lactose intake, and the colon pH of the Test group using

209 BL21: *pet-28a-1* kept relatively stable. Notably, during 2h to 4h, more colon lactose in Test
210 mice was transformed to glucose rather than lactate, as compared to Model mice (Additional
211 file 1: Supplementary methods). Therefore, these results indicate that the tri-stable-switch
212 circuit is able to prevent the mice colon from pH drop caused by excess lactose intake,
213 helping to keep intestinal homeostasis and relieve LI.

214 **The tri-stable-switch circuit helped mice gut microbiota recovery from the effects of**
215 **excess lactose intake**

216 To trace the effects of the engineered bacteria equipped with the tri-stable-switch circuit on
217 mice gut microbiota, we conducted a time-series trial with the high-frequency sampling of
218 mice fecal samples (Additional file 2: Table S7). As was shown in Fig. 4a, four groups of
219 mice (the Untreated group, the Model group, the Control group and the Test group) were
220 under different interventions. The trial lasted for 21 days, divided into the four phases:
221 normal care (Phase I), lactose challenge (Phase II), bacterial treatment (Phase III) and
222 restoration (Phase IV). For Phase I, during which the four groups received normal care, the
223 objective was to stabilize the physical signs and gut microbiota of mice in the four groups.
224 For Phase II, during which lactose was fed to the Model, Control and Test mice, the objective
225 was to investigate the influence of excess lactose. Phase III, in which the BL21: *pet-28a-1*
226 was fed to the Test group while empty-vector-containing BL21: *pet-28a-0* used for mice in
227 the Control group, was used to determine whether the BL21: *pet-28a-1* can alleviate LI. In
228 Phase IV, we intended to observe whether the bacteria caused any side effects in the host
229 mice.

230 Assigning enterotypes is a way to describe and differentiate the variance of gut
231 microbiota, by stratifying gut samples according to their microbial composition [34]. Two
232 enterotypes were firstly identified using all the samples of mice gut microbiota (Fig. 4b),
233 which were statistically validated by CH and SI index (Additional file 2: Table S9). Two
234 enterotypes were evidently different in microbial composition at the taxonomic levels of
235 phylum, class, order, family, and genus (Additional file 2: Table S10). Compared to the
236 samples of enterotype I, the samples of enterotype II displayed lower bacterial richness (P
237 value $< 2.20 \times 10^{-16}$, Mann-Whitney-Wilcoxon test). Additionally, in the lower-richness
238 enterotype II, the proportion of Firmicutes was reduced (P value = 1.60×10^{-13} , Mann-
239 Whitney-Wilcoxon test), while the proportion of Bacteroidetes was increased (P value = 1.16
240 $\times 10^{15}$, Mann-Whitney-Wilcoxon test). The characteristics of these identified mice
241 enterotypes were consistent with those reported in a previous study [35].

242 More interestingly, the dynamics of the mice gut microbiota differed among the four trial
243 groups over the 21-day (four phases) trial (Fig. 4b and c). During Phase I, the microbiota of
244 the gut samples from all the groups were of the enterotype I. At days 5 and 7 (Phase II:
245 lactose challenge), most of the microbiota in the gut samples from the Untreated group
246 trended towards the enterotype II, while the ones in the other groups under lactose treatment
247 mostly remained in enterotype I. On days 11 and 13 (Phase III: bacteria treatment), the
248 microbiota in samples from the Untreated group still trended towards enterotype II, while the
249 ones in the Model and Control groups were restricted to enterotype I. However, the
250 microbiota of the gut samples from the Test group using the BL21: *pet-28a-1* in this phase

251 were mostly in the enterotype II area, with an obvious time lag observed between the Test
252 and Untreated groups. All the microbiota in the gut samples from the four groups finally
253 turned back to enterotype I after normal care during Phase IV. These different dynamic
254 patterns fit well with the data from the mouse weight index recorded during the trials, that the
255 bacteria-treated mice were rescued from LI-induced weight loss (Additional file 1:
256 Supplementary methods, Additional file 2: Table S8). Taken together, these results indicated
257 that the engineered bacteria was able to rescue the gut microbiota in the Test group to the
258 patterns similar to those of the Untreated group.

259 Moreover, at the phylum level (Fig. 4d), when lactose was administrated to mice during
260 Phase II, the proportion of Bacteroidetes was reduced in the Model, Control and Test groups.
261 Nevertheless, during Phase III, the abundance of Bacteroidetes in the Test group was rescued
262 to reach the same level (> 0.8) as the one in the Untreated group during Phase II.
263 Furthermore, a variation pattern at genus level of the Test group was observed to be similar to
264 that of the Untreated group after a time lag as well (Additional file 1: Supplementary
265 methods). We then displayed the network of the top 10 abundant genera (Fig. 4e). The genus
266 *Lactobacillus*, as well as the genus *Bacteroides* was the most abundant (Additional file 2:
267 Table S10) and the most discriminant biomarker (Additional file 1: Supplementary methods)
268 of the enterotype I and enterotype II, respectively. These two genera were observed to be
269 negatively correlated (P value = 1.90×10^{-10} , Kendall's *tau* statistic). Therefore, the growth of
270 the genus *Lactobacillus*, induced by the excess lactose intake might play a role in inhibiting
271 the growth of the genus *Bacteroides* and the dynamic switch to enterotype II in the Phase II

272 and III, which should have happened in a normal condition as observed in the Untreated
273 group. The administration of the BL21: *pet-28a-1* helped the mice of the Test group to
274 remove this inhibition so that their gut microbiota can continue to proceed the enterotype
275 switch in Phase III, just like the mice gut microbiota of the Untreated group have done in
276 Phase II.

277 **Discussion**

278 In this study, we designed a tri-stable-switch circuit with ability of β -GAL accumulation and
279 pH rescue. The engineered bacteria equipped with this circuit can flexibly adapt to the
280 variation of intestinal environment, thus timely digesting lactose and rescuing the intestinal
281 pH drop, along with the recovery of gut microbiota affected by excess lactose intake. We
282 believe using engineered bacteria equipped with this tri-stable-switch circuit can serve as a
283 promising therapeutic method for LI.

284 The tri-stable-switch circuit makes up the defect of non-modified bacteria by not only
285 digesting lactose, but also enabling an additional function of pH rescue. The pH drop caused
286 by fermentation of gut microbiota would not only cause diarrhoea, but also reduce the
287 activity of the intestinal β -GAL and the intestinal homeostasis. Therefore, the tri-stable-
288 switch circuit was designed to response to the signals of pH and lactose concentration, and
289 then dynamically switch between two functional states: accumulation of β -GAL and pH
290 rescue. The accumulation of β -GAL can help to digest lactose with high efficiency;
291 meanwhile the pH rescue function helps to keep the intestinal homeostasis, giving engineered

292 bacteria with this circuit better adaptability to intestinal environment than non-modified

293 bacteria. These two functions have been confirmed in our *in vitro* and *in vivo* test.

294 Interestingly, in a 21-days *in vivo* mice trial, the engineered bacteria with the tri-stable-

295 switch circuit was demonstrated to be able to recover the mice gut microbiota from the

296 effects of excess lactose intake. During the trial, mice gut microbiota was influenced and

297 could provide feedback to the environmental changes: The fermentation of unabsorbed

298 lactose by gut microbiota produced acids and gas, leading to pH drop in the colon. This

299 change of the environment in the colon would affect the gut microbiota in return. On the

300 other hand, colonization of engineered bacteria affected the microbiota through microbial

301 interactions, and its expressed products would also influence the intestinal environment. To

302 explore the patterns of gut microbiota variation, we firstly identified two enterotypes based

303 on the stratification of mice gut microbiota, and then we used the boundary of these two

304 enterotypes as a threshold to identify the degree of variation in the microbiota. The most

305 significant difference between the Untreated groups and other groups was found during Phase

306 II (lactose challenge): when most of the mice microbiota samples in the Untreated group

307 trended towards the enterotype II area, the ones from other groups seemed to be suppressed

308 in the enterotype I area. This suppression might be caused by the intake of excess lactose.

309 However, the suppression on the Test samples was subsequently removed by the feeding of

310 our engineered bacteria during Phase III (bacteria treatment).

311 This study also has limitations. First, this study mainly underscores the design of the tri-

312 stable-switch circuit and the confirmation of its functionality. Hence, for this purpose, the

313 used *Escherichia coli* BL21 strain would be proper for functionality confirmation of a
314 prototype rather than for the therapeutic intention. To apply this tri-stable-switch circuit to
315 human still needs more sophisticated studies to find a proper chassis and ensure safety.
316 Second, it has already been realized that the pH of the mice colon is lower than that of human
317 colon. The switch of the tri-stable-switch circuit is completed in a pH range close to a normal
318 condition, which better fits in human intestine. Nevertheless, in the *in vitro* experiment under
319 a broad range of pH set, we have observed that it can still work well under a lower pH
320 condition during the gradual process of the switch. Thirdly, the 16S rRNA gene sequencing
321 cannot classify some potentially important gut microbes to the species level, the strain level,
322 and the gene level. Nevertheless, the observed macroscopic trend of the gut microbiota
323 variation has confirmed the recovery effects of the circuit, though the explanation of this
324 trend still needs further investigations.

325

326 **Methods**

327 **Experimental design**

328 The gene sequences of the tri-stable-switch circuit were firstly synthesized by Integrated
329 DNA Technologies and assembled by 3A assembly. The 3A-assembled intermediate parts
330 were then assembled using In-Fusion. The circuit was transformed into the *E. coli* BL21 for
331 the following *in vitro* and *in vivo* experiments. *In vitro* experiments were designed to
332 investigate on the variation of pH value, variation of β -galactosidase (β -GAL) activity, and
333 variation of l-lactate dehydrogenase (L-LDH) activity of the bacterial culture under different

334 pH levels. *In vivo* experiments were designed to investigate on the variation of pH value of
335 the mice colon after intake of excess lactose. In addition, the sets of mice with or without
336 administration of the engineered bacteria were used to observe the ability of pH rescue of the
337 tri-stable-switch circuit. Another 21-days *in vivo* experiment was used to investigate on the
338 gut microbiota variation of the mice after intake of excess lactose. The sets of mice with or
339 without administration of the engineered bacteria were used to observe the effects of the tri-
340 stable-switch circuit on gut microbiota.

341 The details of the circuit construction such as 3A assembly and fluorescence detection, the
342 details of the *in vitro* experiments such as media preparation and measurements of enzyme
343 activity, and the details of the *in vivo* experiments such as mice operations, 16S rRNA gene
344 sequencing and microbiome analysis are available in the Supplementary Materials and
345 Methods.

346 **Statistical Analysis**

347 For categorical metadata and enterotype comparisons, samples were pooled into bins
348 (Enterotype I/Enterotype II, Day 3/Day 5/Day 7..., etc.) and significant features were
349 identified using Mann-Whitney-Wilcoxon Test with Benjamini and Hochberg correction of *P*
350 values.

351

352 **Additional files**

353 **Additional file 1: Supplementary methods**

354 The detailed designs and supplementary results of experiments including circuit construction,
355 tri-stable switch confirmation, tri-stable circuit modelling, the *in vitro* experiment, the *in vivo*
356 experiment, and the gut microbiota detection.

357 **Additional file 2: Supplementary tables**

358 The supplementary table 1 to 10 used for the manuscript and additional file 1.

359 **Additional file 3: The plasmid profile of *pet-28a-1*.**

360 **Additional file 4: The plasmid profile of *pet-28a-0*.**

361

362 **Ethics approval and consent to participate**

363 Not applicable

364

365 **Consent for publication**

366 Not applicable

367

368 **Availability of data and material**

369 The datasets generated and analyzed during the current study are available in the short read
370 archive (SRA) section of National Center for Biotechnology Information, under accession
371 SRP152703.

372

373 **Competing interests**

374 The authors have declared no competing interests.

375

376 **Funding**

377 This project was supported by grants from the Ministry of Science and Technology of
378 People's Republic of China (Grant No. 2018YFC0910502), the National Natural Science
379 Foundation of China (Grant No. NSFC-31871334 and NSFC-31671374), the Teaching
380 Research Program from Hubei Province of China (Grant No. 2016071), and the National
381 Undergraduate Training Programs for Innovation and Entrepreneurship (Grant No.
382 201710487069) from HUST and the Ministry of Education of China.

383

384 **Authors' contributions**

385 MY. C., ZY. C., YJ. Y., Y. Z. and K. N. designed the experiments. JM. L. and YG. T.
386 conducted the DNA extraction and sequencing. MY. C., ZY. C., YY. Y., WJ. L., ZY. G., JY.
387 Q., Z. Z., L. D., YF. M., and RH. L. conducted the plasmid constructions, fluorescence
388 detection, and data analysis. MY. C., ZY. C., YY. Y, CX. P., and YH. L. conducted the *in*
389 *vitro* and *in vivo* experiments. MY. C., ZY. C., Y. Z. and K. N. wrote and revised the
390 manuscript.

391

392 **Acknowledgements**

393 We thank all that have provided assistance for iGEM team HUST-China in iGEM 2016.

394

395 **References**

- 396 1. Storhaug CL, Fosse SK, Fadnes LT. Country, regional, and global estimates for lactose
397 malabsorption in adults: A systematic review and meta-analysis. *Lancet Gastroenterol*
398 *Hepatol.* 2017;2:738–46.
- 399 2. Fassio F, Facioni MS, Guagnini F. Lactose maldigestion, malabsorption, and intolerance:
400 A comprehensive review with a focus on current management and future perspectives.
401 *Nutrients.* 2018;10.
- 402 3. de Vrese M, Stegelmann A, Richter B, Fenselau S, Laue C, Schrezenmeir J. Probiotics--
403 compensation for lactase insufficiency. *Am J Clin Nutr.* 2001;73:421s–9s.
- 404 4. Heyman M. Effect of lactic acid bacteria on diarrheal diseases. *J Am Coll Nutr.*
405 2000;19:137s–46s.
- 406 5. Bohmer CJ, Tuynman HA. The effect of a lactose-restricted diet in patients with a
407 positive lactose tolerance test, earlier diagnosed as irritable bowel syndrome: A 5-year
408 follow-up study. *Eur J Gastroenterol Hepatol.* 2001;13:941–4.
- 409 6. Shaukat A, Levitt MD, Taylor BC, MacDonald R, Shamliyan TA, Kane RL, et al.
410 Systematic review: Effective management strategies for lactose intolerance. *Ann Intern Med.*
411 2010;152:797–803.
- 412 7. Wilder-Smith CH, Olesen SS, Materna A, Drewes AM. Predictors of response to a low-
413 fodmap diet in patients with functional gastrointestinal disorders and lactose or fructose
414 intolerance. *Aliment Pharmacol Ther.* 2017;45:1094–106.

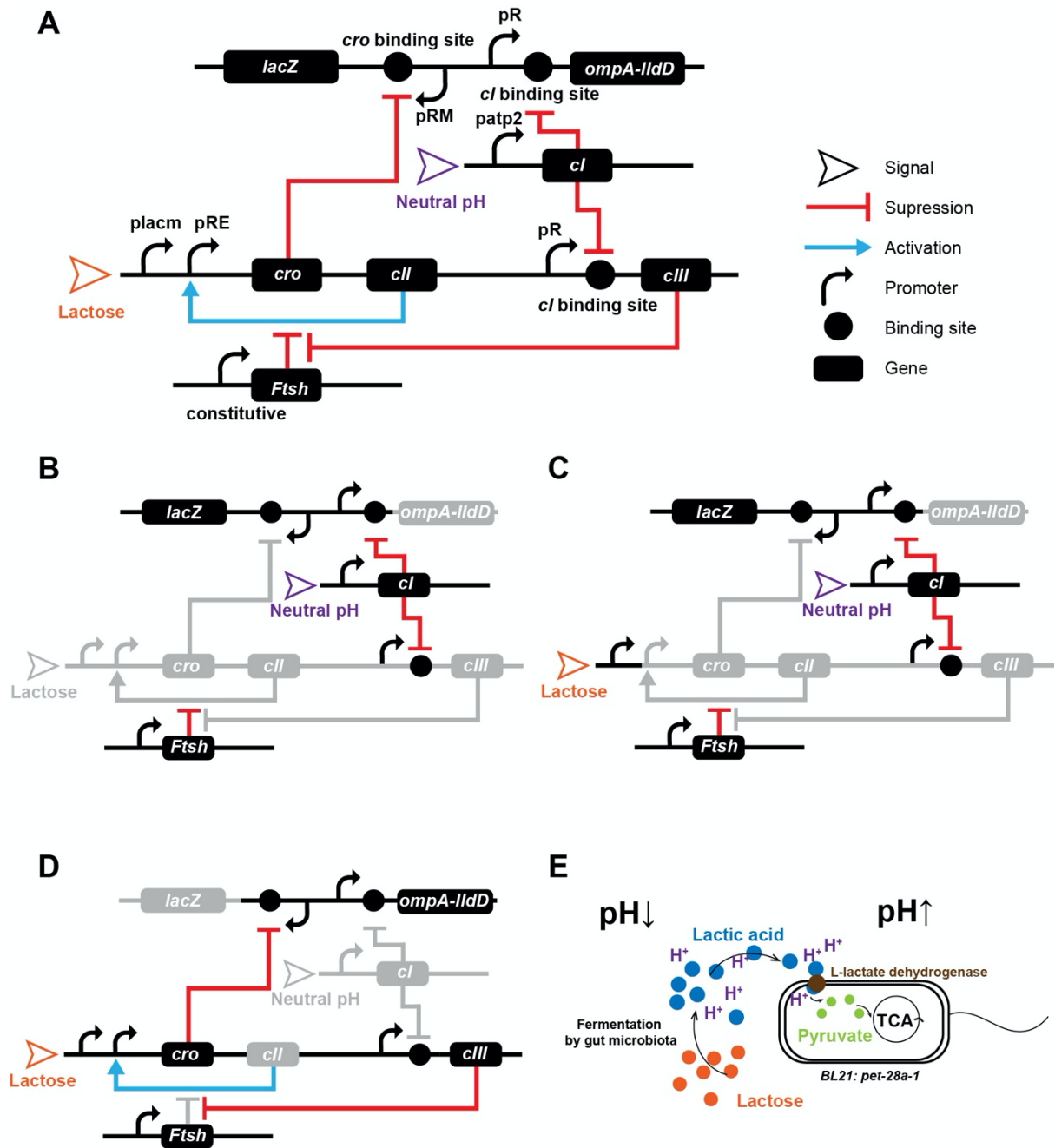
- 415 8. Azcarate-Peril MA, Ritter AJ, Savaiano D, Monteagudo-Mera A, Anderson C, Magness
416 ST, et al. Impact of short-chain galactooligosaccharides on the gut microbiome of lactose-
417 intolerant individuals. *Proc Natl Acad Sci U S A*. 2017;114:E367–e75.
- 418 9. Ianiro G, Pecere S, Giorgio V, Gasbarrini A, Cammarota G. Digestive enzyme
419 supplementation in gastrointestinal diseases. *Curr Drug Metab*. 2016;17:187–93.
- 420 10. Ojetti V, Gigante G, Gabrielli M, Ainora ME, Mannocci A, Lauritano EC, et al. The
421 effect of oral supplementation with *Lactobacillus reuteri* or *Lactase* in lactose intolerant
422 patients: Randomized trial. *Eur Rev Med Pharmacol Sci*. 2010;14:163–70.
- 423 11. Almeida CC, Lorena SL, Pavan CR, Akasaka HM, Mesquita MA. Beneficial effects of
424 long-term consumption of a probiotic combination of *Lactobacillus casei shirota* and
425 *Bifidobacterium breve yakult* may persist after suspension of therapy in lactose-intolerant
426 patients. *Nutr Clin Pract*. 2012;27:247–51.
- 427 12. He T, Priebe MG, Zhong Y, Huang C, Harmsen HJ, Raangs GC, et al. Effects of yogurt
428 and bifidobacteria supplementation on the colonic microbiota in lactose-intolerant subjects. *J*
429 *Appl Microbiol*. 2008;104:595–604.
- 430 13. Oak SJ, Jha R. The effects of probiotics in lactose intolerance: A systematic review. *Crit*
431 *Rev Food Sci Nutr*. 2019;59:1675–83.
- 432 14. Tomizawa M, Tsumaki K, Sone M. Characterization of the activity of beta-galactosidase
433 from *Escherichia coli* and *Drosophila melanogaster* in fixed and non-fixed *Drosophila* tissues.
434 *Biochim Open*. 2016;3:1–7.

- 435 15. Juajun O, Nguyen TH, Maischberger T, Iqbal S, Haltrich D, Yamabhai M. Cloning,
436 purification, and characterization of beta-galactosidase from bacillus licheniformis dsm 13.
437 Appl Microbiol Biotechnol. 2011;89:645–54.
- 438 16. Hilton IB, Gersbach CA. Enabling functional genomics with genome engineering.
439 Genome Res. 2015;25:1442–55.
- 440 17. Saeidi N, Wong CK, Lo TM, Nguyen HX, Ling H, Leong SS, et al. Engineering
441 microbes to sense and eradicate pseudomonas aeruginosa, a human pathogen. Mol Syst Biol.
442 2011;7:521.
- 443 18. Danino T, Prindle A, Kwong GA, Skalak M, Li H, Allen K, et al. Programmable
444 probiotics for detection of cancer in urine. Sci Transl Med. 2015;7:289ra84.
- 445 19. Hwang IY, Koh E, Wong A, March JC, Bentley WE, Lee YS, et al. Engineered probiotic
446 escherichia coli can eliminate and prevent pseudomonas aeruginosa gut infection in animal
447 models. Nat Commun. 2017;8:15028.
- 448 20. Li J, Zhang W, Wang C, Yu Q, Dai R, Pei X. Lactococcus lactis expressing food-grade
449 beta-galactosidase alleviates lactose intolerance symptoms in post-weaning balb/c mice. Appl
450 Microbiol Biotechnol. 2012;96:1499–506.
- 451 21. Zhang W, Wang C, Huang C, Yu Q, Liu H, Zhang C, et al. Construction and expression
452 of food-grade beta-galactosidase gene in lactococcus lactis. Curr Microbiol. 2011;62:639–44.
- 453 22. Rajkumar AS, Liu G, Bergenholm D, Arsovska D, Kristensen M, Nielsen J, et al.
454 Engineering of synthetic, stress-responsive yeast promoters. Nucleic Acids Res.
455 2016;44:e136.

- 456 23. Ptashne M. A genetic switch: Gene control and phage. Lambda. 1986.
- 457 24. Evans DF, Pye G, Bramley R, Clark AG, Dyson TJ, Hardcastle JD. Measurement of
458 gastrointestinal pH profiles in normal ambulant human subjects. *Gut*. 1988;29:1035–41.
- 459 25. Schubert RA, Dodd IB, Egan JB, Shearwin KE. Cro's role in the *ci* cro bistable switch is
460 critical for λ 's transition from lysogeny to lytic development. *Genes Dev*.
461 2007;21:2461–72.
- 462 26. Halder S, Datta AB, Parrack P. Probing the antiprotease activity of λ ciiii, an
463 inhibitor of the *Escherichia coli* metalloprotease Hflb (FtsH). *J Bacteriol*. 2007;189:8130–8.
- 464 27. Pocanschi CL, Popot JL, Kleinschmidt JH. Folding and stability of outer membrane
465 protein A (OmpA) from *Escherichia coli* in an amphipathic polymer, amphipol 8-35. *Eur*
466 *Biophys J*. 2013;42:103–18.
- 467 28. Futai M, Kimura H. Inducible membrane-bound L-lactate dehydrogenase from *Escherichia*
468 *coli*. Purification and properties. *J Biol Chem*. 1977;252:5820–7.
- 469 29. Kimura H, Futai M. Effects of phospholipids on L-lactate dehydrogenase from membranes
470 of *Escherichia coli*. Activation and stabilization of the enzyme with phospholipids. *J Biol*
471 *Chem*. 1978;253:1095–110.
- 472 30. Herzig S, Raemy E, Montessuit S, Veuthey JL, Zamboni N, Westermann B, et al.
473 Identification and functional expression of the mitochondrial pyruvate carrier. *Science*.
474 2012;337:93–6.
- 475 31. Kristoficova I, Vilhena C, Behr S, Jung K. Btst, a novel and specific pyruvate/h⁽⁺⁾
476 symporter in *Escherichia coli*. *J Bacteriol*. 2018;200.

- 477 32. Deng Y, Ma N, Zhu K, Mao Y, Wei X,Zhao Y. Balancing the carbon flux distributions
478 between the tca cycle and glyoxylate shunt to produce glycolate at high yield and titer in
479 escherichia coli. *Metab Eng.* 2018;46:28–34.
- 480 33. McConnell EL, Basit AW,Murdan S. Measurements of rat and mouse gastrointestinal ph,
481 fluid and lymphoid tissue, and implications for in-vivo experiments. *J Pharm Pharmacol.*
482 2008;60:63–70.
- 483 34. Arumugam M, Raes J, Pelletier E, Le Paslier D, Yamada T, Mende DR, et al.
484 Enterotypes of the human gut microbiome. *Nature.* 2011;473:174–80.
- 485 35. Hildebrand F, Nguyen TL, Brinkman B, Yunta RG, Cauwe B, Vandenabeele P, et al.
486 Inflammation-associated enterotypes, host genotype, cage and inter-individual effects drive
487 gut microbiota variation in common laboratory mice. *Genome Biol.* 2013;14:R4.
- 488

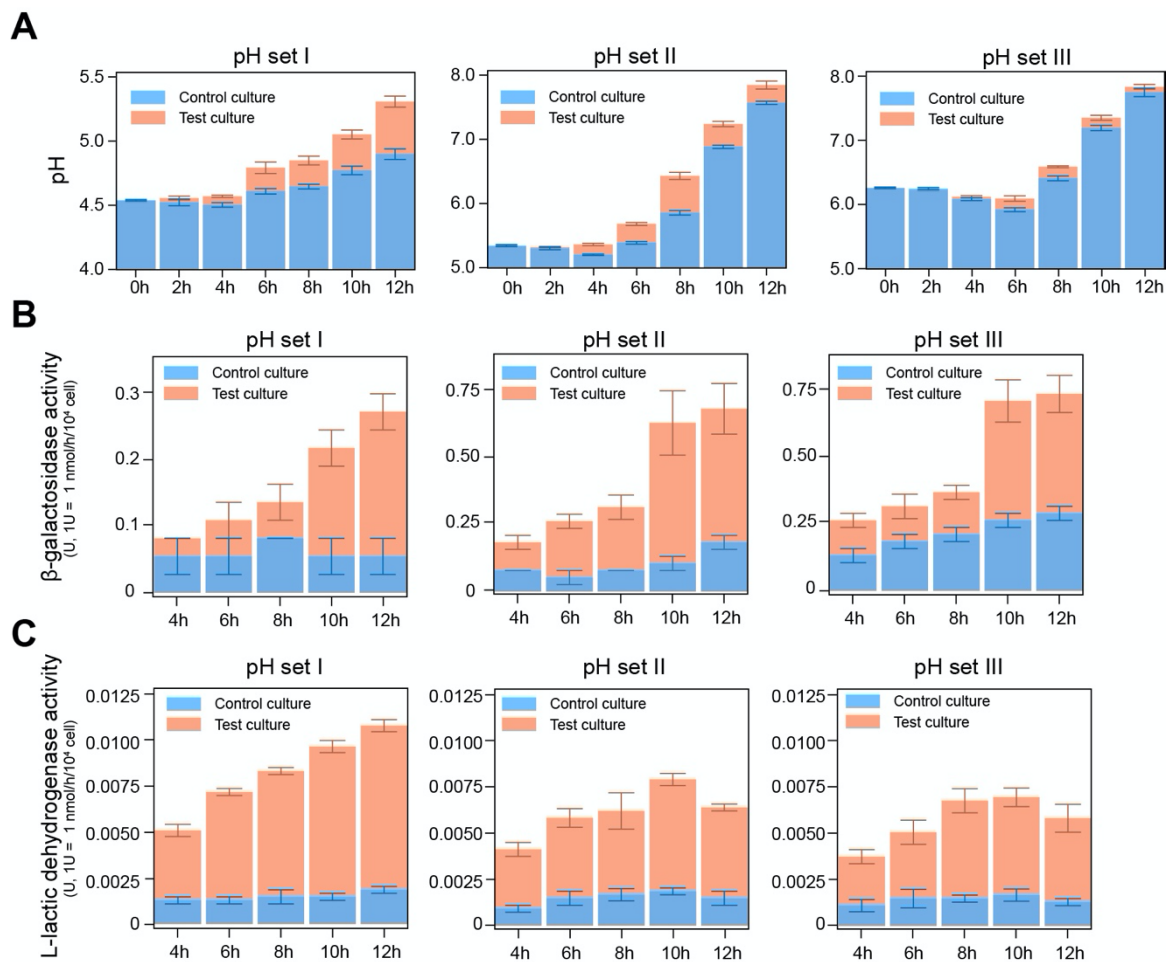
489 **Figures**



490

491 **Fig. 1** The tri-stable-switch circuit can switch between two functionalities in response to
 492 environmental change. **a** The design diagram of the tri-stable switch circuit. Parts of the
 493 circuit are derived from the bacteriophage *lambda*. The two promoters *placm* and *patp2* are
 494 selected for sensing the lactose and pH signals, respectively. **b** When the BL21: *pet-28a-1*
 495 colonizes in the colon with a neutral pH, *lacZ* is stably expressed and accumulates β-GAL

496 intracellularly. **c** When a flux of unabsorbed lactose occurs in the colon, the system switches
 497 to a transition state in response to lactose and pH signals. The expression of *ompA-lldD* for L-
 498 lactate dehydrogenase is strengthened and the expression of *lacZ* is weakened. **d** The system
 499 then focuses on expression of *ompA-lldD*. **e** The fermentation of lactose by gut microbiota
 500 causes pH drop, while the expressed L-lactate dehydrogenase can transform lactic acid into
 501 pyruvate, thus recovering the pH. The pyruvate then permeates into the cell for TCA
 502 pathway.
 503

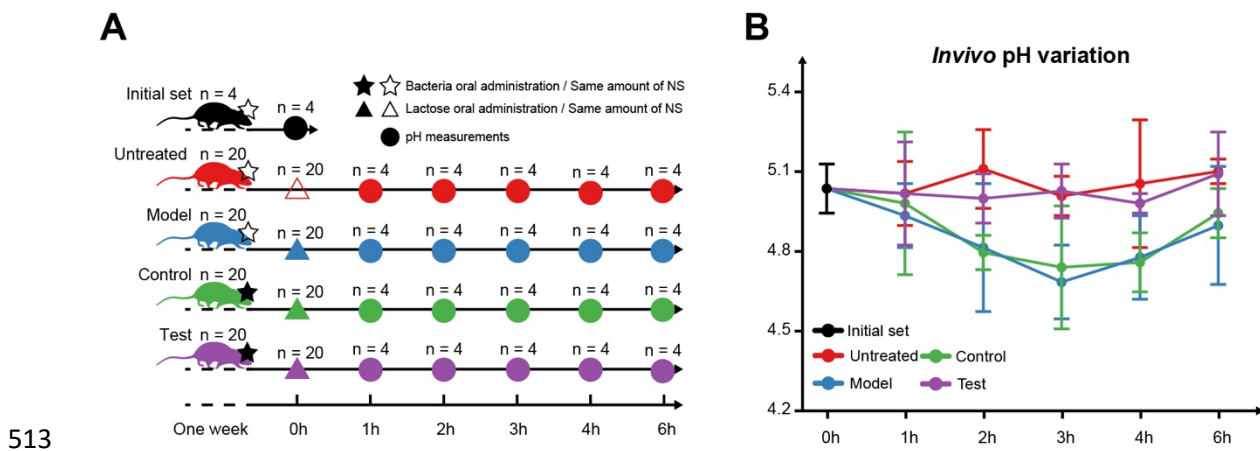


504

505 **Fig. 2** The tri-stable-switch circuit was efficient under a range of pH simulation *in vitro*. **a**

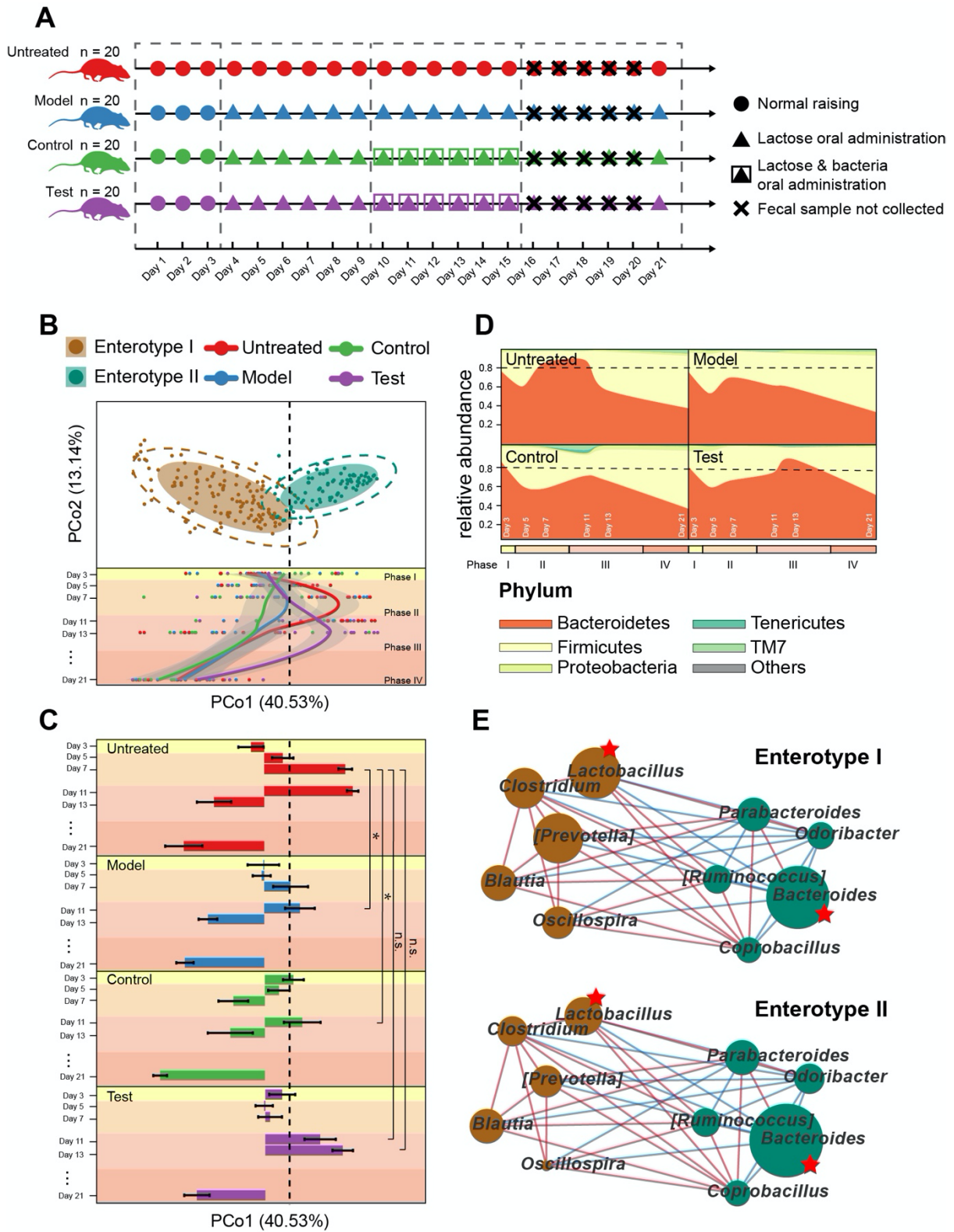
506 The mean \pm s.e.m. of pH variation during 12 hrs of the cultures of the bacteria grown at

507 different set of pH. **b** The mean \pm s.e.m. of β -GAL activity during 12 hrs of the cultures of
 508 the bacteria grown at different set of pH. **c** The mean \pm s.e.m. of l-lactate dehydrogenase
 509 activity during 12 hrs of the cultures of the bacteria grown at different set of pH. In all panels,
 510 the control culture (BL21: *pet-28a-0*) is colored in orange, while the test culture (BL21: *pet-*
 511 *28a-1*) is colored in blue.
 512



513
 514 **Fig. 3 The tri-stable-switch circuit helped mice to recover the pH drop caused by excess**
 515 **lactose intake. a** Five groups of mice including the Initial set (n = 4), the Untreated group (n
 516 = 20), the Control group (n = 20), the Test group (n = 20) were firstly subjected to different
 517 operations in one week. Mice in the Control group and the Test group were daily
 518 administrated with bacteria (BL21: *pet-28a-0* in the Control group, BL21: *pet-28a-1* in the
 519 Test group. OD₆₀₀ = 1) in a total volume of 0.3 mL 0.9% NS suspension. Other groups were
 520 daily administrated with the same volume of 0.9% NS. At the time point of 0h, mice of the
 521 Initial set were killed for pH measures, and mice of other four groups were administrated
 522 with the lactose solution (12 mg of lactose per 20 g of body weight). In the following 6 hrs,
 523 four mice of each group were killed at each time point for pH measures. **b** The mean \pm s.d. of

524 pH variation of the mice colon during 6 hrs. The Initial set is designated as the initial point of
 525 four other groups. The pH variation of different groups is coloured differently.



526

527 **Fig. 4** The tri-stable-switch circuit helped mice gut microbiota recovery from the effects of
528 excess lactose intake. **a** The design of the mice trial for gut microbiota profiling (Detailed
529 operations are available in the Additional file 1: Supplementary methods). **b** Top panel:
530 Individual mice gut microbiota composition in the Untreated group (54 samples), Model
531 group (55 samples), Control group (53 samples), and Test group (59 samples), stratified into
532 two enterotypes and plotted on a JSD PCoA plot. The shaded ellipses represent an 80%
533 confidence interval. The dotted ellipse borders represent a 95% confidence interval. Bottom
534 panel: The gut microbiota samples are plotted according to their collection date on the y axis
535 over 21 days, and their position on the x axis is plotted according to their first principal
536 coordinate in the JSD-based PCoA (top panel). A Loess regression is applied to these points
537 using the collection date and PCo1 coordinates, and the curves are plotted in different colors
538 according to their groups, with a 95% pointwise confidence interval band in the gray shade.
539 The dashed line is plotted to divide the area of the two enterotypes. **c** The mean \pm s.e.m. of
540 PCo1 coordinates from the four trial groups across 21 days. The dashed line represents the
541 position on the x axis that divides the areas of the two enterotypes. A delayed shift to
542 Enterotype II was observed in the Test group. *P < 0.05, **P < 0.01, ***P < 0.001; ns, not
543 significant. Mann-Whitney-Wilcoxon Test. **d** The taxonomic variation of the mean relative
544 abundance at the phylum level among four groups over the 21 days are shown in a stream
545 graph. The dashed line represents a mean relative abundance of 0.8. **e** The network is
546 constructed using the top ten abundant genera, based on the Kendall correlation with p value
547 < 0.5 (Kendall's *tau* statistic test) and q value < 0.5 (Benjamini and Hochberg corrections).

548 The size of the node represents the mean abundance among enterotype I samples (top panel)
549 or enterotype II samples (bottom panel). The color of the node represents the enterotype
550 where the genus is more abundant. The asterisk refers to the most discriminant genus. The
551 color of the edge represents the positive (red) or negative (blue) correlation.
552